Partial Miscibility Behavior of the Methane + Ethane + *n*-Docosane and the Methane + Ethane + *n*-Tetradecylbenzene Ternary Mixtures

Adisak Jangkamolkulchai and Kraemer D. Luks*

Department of Chemical Engineering, University of Tulsa, Tulsa, Oklahoma 74104-3189

The liquid–liquid–vapor (LLV) partial miscibility behavior of the mixtures methane + ethane + *n*-docosane and methane + ethane + *n*-tetradecylbenzene is experimentally studied by use of a visual cell (stoichiometric) technique. Phase compositions and molar volumes of the three fluid phases in equilibrium are reported as functions of temperature and pressure within the regions. Also presented are LLV phase equilibria data for the binary system ethane + *n*-tetradecylbenzene. The two ternary systems have constituent binary mixtures that exhibit LLV partial miscibility. In pressure–temperature space, the addition of the third component, methane, promotes growth of the three-phase LLV region from the binary LLV locus toward the vapor pressure curve of methane. The three-phase regions of both ternary systems are bounded from above by an upper critical end point (L–L=V) locus, from below by a lower critical end point (L=L–V) locus, and at low temperatures by a four-phase (SLLV) locus.

Introduction

The authors have undertaken an extensive study of phase equilibria behavior and liquid–liquid–vapor (LLV) immiscibility phenomena in prototype rich gas + oil mixtures. "Rich gas", a mixture of methane + ethane + propane that has been separated from a live oil, is sometimes reinjected into reservoirs to enhance the recovery of the remaining oil. The purposes of the study are to map out the patterns of multiphase equilibria of these prototype mixtures in thermodynamic phase space and to generate a phase equilibria data base that would be useful for developing and testing equation-of-state models used to predict phase equilibria in and near regions of LLV immiscibility.

There is limited immiscibility observed in the homologous series of binary mixtures of *n*-paraffins + methane, ethane, or propane. Partial miscibility has been observed in the mixtures methane + *n*-hexane (*1*) and methane + *n*-heptane (*2*, *3*). *n*-Pentane is completely miscible with methane, while *n*-octane and higher members of the homologous series of *n*-paraffins are too molecularly dissimilar to methane to have a LLV region. Instead, a solid phase of the *n*-paraffin forms before immiscibility occurs, and two separate LV regions are created. The thermodynamic phase space topography of systems exhibiting multiphase equilibria behavior has been reviewed by Luks and Kohn (*4*).

LLV immiscibility is seen in mixtures of ethane + *n*-paraffins ranging from *n*-octadecane to *n*-pentacosane (*5*–*12*). For carbon numbers 18–23, the LLV extends from a lower critical end point L=L–V (LCEP) to an upper critical end point L–L=V (type K point), in the same manner as methane + *n*-hexane. For carbon numbers 24 and 25, the LLV locus is terminated below by the formation of a solid phase of the *n*-paraffin as a four-phase point SLLV (quadruple or Q point) as with methane + n-heptane.

Recently, the authors have studied the liquid–liquid–vapor phase equilibria for the mixtures ethane + *n*-alkylbenzene homologous series (*13*). *n*-Nonylbenzene was found to be the first member of this series to exhibit LLV immiscibility with ethane. For the *n*-alkylbenzene homologous series up to at least *n*-tetradecylbenzene, the LLV loci extend from a LCEP to a K point. Because of the lower melting points of the *n*-alkylbenzene series (compared to the *n*-paraffin series, given the same carbon number), the LLV immiscibility of the ethane + *n*-alkylbenzene homologous series will persist to higher carbon numbers. Miller and Luks (*14*) have recently estimated the upper immiscibility limits of the homologous series ethane + *n*-alkylbenzenes.

Given a LLV-immiscible binary system of a rich gas (solvent) component + hydrocarbon (solute), the addition of a third component generates a LLV surface in thermodynamic phase space, with the binary LLV locus as one boundary. The geometric nature of the ternary surface is generally governed by the properties of the third component relative to the components of the immiscible binary system (*4*, *15*). In this study, when methane is added to the ethane-rich binary immiscible mixture, the three-phase LLV region develops toward the vapor pressure curve of methane. In essence, the location of the LLV region in pressure–temperature space is governed by the presence of the methane and the ethane, given a hydrocarbon solute of low volatility.

Herein, the phase equilibria of the ternary mixtures methane + ethane + *n*-docosane and methane + ethane + *n*-tetradecylbenzene were studied by use of a visual cell (stoichiometric) experimental technique. The purpose of this study is to understand the effect of the third component, methane, on the phase equilibria behavior within the three-phase LLV region developed with different ethane-rich immiscible binary mixtures (containing paraffinic and aromatic hydrocarbons, respectively). Given that the melting point of *n*-tetradecylbenzene (9.68 °C) is lower than that of *n*-docosane (43.59 °C), one would expect, upon adding methane, the three-phase LLV region of the system methane + ethane + *n*-tetradecylbenzene to be expanded toward the vapor pressure curve of methane to lower temperatures than for the system methane + ethane + *n*-docosane before the quadruple point (SLLV) locus occurs. We have experimentally mapped out the boundaries of the LLV regions in the pressure–temperature space and have detailed the compositions and molar volumes of the three fluid phases along three isotherms (5, 15, and 25 °C) for the mixture methane + ethane + *n*-tetradecylbenzene and along two isotherms (25 and 30 °C) for the mixture methane + ethane + *n*-docosane. We also report the temperature, pressure, phase compositions, and molar volumes of the two liquid phases along the LLV locus of the binary mixture ethane + *n*-tetradecylbenzene. A similar study of the binary mixture ethane + *n*-docosane was reported earlier (*10*).

Experimental Apparatus and Procedures

A description of the apparatus and some of the experimental procedures have been given in earlier papers by Fall, Fall, and

---

*To whom correspondence should be addressed.

0021-9568/89/1734-0092$01.50/0

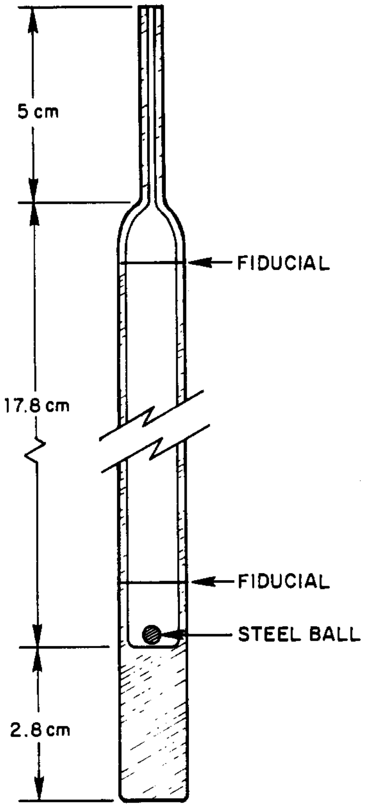

Figure 1. The glass equilibrium visual cell.

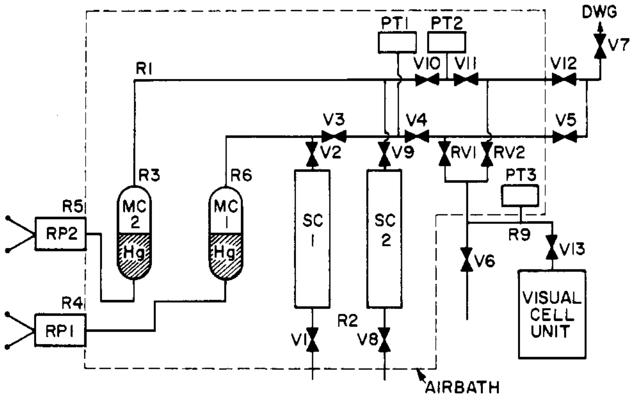

Figure 2. Schematic diagram of the experimental apparatus.

Luks (*16–18*). We review and update this information here for the convenience of the reader. The data are taken using a stoichiometric approach, with the experimental phase equilibria system being contained in a glass visual cell, illustrated in Figure 1. The internal volume of the glass cell is typically 7–8 mL, and phase volumes within the cell can be accurately measured to ±0.005 mL with a cathetometer, once the volume correspondence of height relative to a fiducial mark on the cell is calibrated. The contents of the cell can be stirred to achieve phase equilibria by using a steel ball manually actuated by an overriding magnet.

The visual cell is attached to a gas feed line, in a visual cell unit (see Figure 2), with a standard Swagelok 1/4-in. stainless steel fitting with a Teflon ferrule to achieve the metal-to-glass seal. A cell holder is required to keep the cell from slipping longitudinally. The visual cell unit consists of a stirred bath contained in an unsilvered 4-L Dewar vessel. The temperature of the bath can be readily controlled to at least ±0.01 K by manipulating heating and cooling devices.

Table I. Temperature and Pressure Raw Data for the Boundary Loci of Methane + Ethane + *n*-Docosane

temp, K	press., bar	temp, K	press., bar
	K Points		
308.04[a]	51.19	302.16	54.52
307.27	51.61	300.16	55.60
305.71	52.48	297.97	56.77
304.14	53.42		
	Q Points		
295.06	45.99	295.90	52.37
295.25	47.31	296.20	54.59
295.54	49.81	296.45	56.55
	LCEP Points		
300.98[b]	43.97	297.40	44.60
300.37	44.07	295.88	44.81
298.93	44.37		

[a] Binary K point. [b] Binary LCEP point.

Table II. Temperature and Pressure Raw Data for the Boundary Loci of Methane + Ethane + *n*-Tetradecylbenzene

temp, K	press., bar	temp, K	press., bar
	K Points		
307.98[a]	51.04	293.66	58.83
306.09	52.18	290.18	60.43
304.14	53.37	286.54	61.98
302.13	54.45	283.37	63.18
299.15	56.06	278.75	64.76
296.17	57.65	275.09	65.67
	Q Points		
268.75	36.14	271.14	50.10
269.34	40.59	271.82	53.91
270.13	44.46	271.96	58.08
270.33	46.63	272.62	61.34
	LCEP Points		
292.40[b]	36.48	283.49	36.49
291.68	36.48	280.58	36.12
290.20	36.49	277.56	35.80
287.61	36.48	274.25	35.38
285.21	36.49	270.71	34.82

[a] Binary K point. [b] Binary LCEP point.

The air-bath section in Figure 2, thermostated at approximately 50 °C to ±0.1 K, contains a dual gas storage and delivery system. One can deliver gases, at constant temperature and pressure, to the visual cell with 100-cm^3 Ruska positive displacement pumps (RP1, RP2) which drive the gases with a mercury "piston" from solvent gas bombs (MC1, MC2) to the visual cell. This gas delivery system is separated from the feed line to the visual cell by regulating valves (RV1 and RV2). The amount of gas that passes the regulating valves can be determined by the advance of the Ruska pumps. The temperatures of the gases are determined by platinum-resistance surface temperature sensors (R1, R2, R3, etc.) which are calibrated to ±0.1 K. The pressures of the gases in the bombs are determined by pressure transducers (PT1 and PT2). In case of a need to provide more gas to the bombs MC1 and MC2, additional gases are stored in larger storage bombs SC1 and SC2.

The procedure for studying a ternary liquid–liquid–vapor isotherm is as follow. An empty volume-calibrated visual cell is tared. Then the heavy hydrocarbon species, i.e., *n*-docosane or *n*-tetradecylbenzene, is added as a liquid to the cell by a syringe, and the visual cell is reweighed. The cell is placed in the Dewar bath in the cell holder and attached to the unit at the feed line. Without stirring the liquid hydrocarbon phase, the vapor space of the cell and the feed line is flushed several times with the first gas to be added. For this study, ethane is used for flushing. Upon completion of flushing, the Ruska pumps are

Table III. Pressure, Phase Compositions, and Molar Volumes for the Liquid-Liquid-Vapor Region of Methane + Ethane + n-Docosane

	L_1 phase			L_2 phase			V phase	
	mole fracn			mole fracn				
press., bar	C_1	C_2	mol vol, mL/(g·mol)	C_1	C_2	mol vol, mL/(g·mol)	mole fracn C_2	mol vol, mL/(g·mol)
Temperature = 25 °C (298.15 K)								
44.49[a]								
46.88	0.0262	0.9095	89.3	0.0352	0.9546	86.8	0.9325	229.9
47.92	0.0304	0.9007	90.2	0.0426	0.9490	88.0	0.9217	221.3
48.95	0.0345	0.8920	91.0	0.0497	0.9432	89.1	0.9111	213.3
49.99	0.0381	0.8844	92.2	0.0573	0.9367	90.3	0.9018	205.2
51.02	0.0415	0.8769	93.5	0.0649	0.9300	91.5	0.8929	197.5
52.06	0.0450	0.8699	94.4	0.0723	0.9234	93.1	0.8847	188.8
53.09	0.0486	0.8634	95.3	0.0805	0.9159	95.2	0.8780	179.8
54.12	0.0529	0.8547	96.4	0.0883	0.9091	97.1	0.8723	169.7
55.16	0.0564	0.8477	97.3	0.0976	0.9002	100.4	0.8683	159.1
56.67[b]								
Temperature = 30 °C (303.15 K)								
45.98[c]		0.9385	91.2		0.9915	87.9		
47.35	0.0053	0.9252	92.1	0.0092	0.9837	90.2	0.9871	215.4
47.92	0.0077	0.9204	92.7	0.0129	0.9807	91.1	0.9806	210.3
48.61	0.0106	0.9145	93.2	0.0173	0.9771	92.2	0.9723	203.9
49.10	0.0126	0.9108	93.7	0.0202	0.9747	93.1	0.9677	197.0
49.64	0.0147	0.9068	94.1	0.0236	0.9717	94.0	0.9625	192.5
50.19	0.0168	0.9026	94.6	0.0271	0.9686	95.1	0.9573	187.6
51.02	0.0199	0.8965	95.3	0.0331	0.9634	97.1	0.9506	180.0
51.71	0.0225	0.8916	95.9	0.0382	0.9588	99.3	0.9453	173.3
52.43	0.0252	0.8867	96.2	0.0436	0.9539	102.1	0.9404	166.3
53.97[b]								

[a] LCEP point. [b] K point. [c] Interpolated binary data from ref *10*.

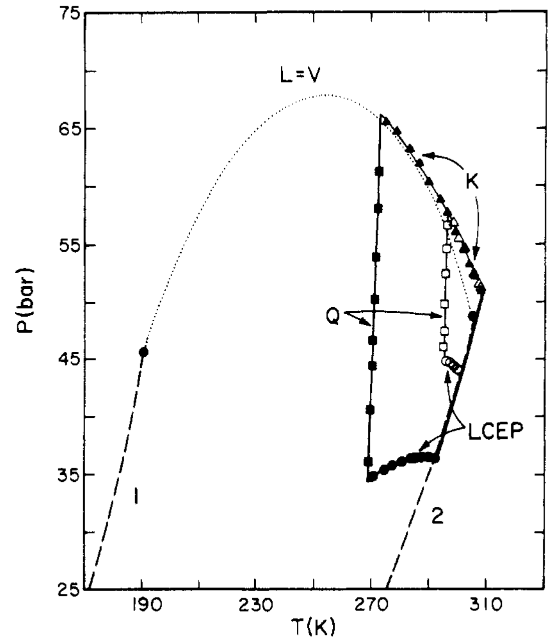

Figure 3. Liquid–liquid–vapor regions of the mixtures methane + ethane + *n*-docosane (open symbols) and methane + ethane + *n*-tetradecylbenzene (filled symbols) in pressure–temperature space. Also shown are the critical point locus for the binary mixture methane + ethane (dotted curve) and the vapor pressure curves of pure methane and ethane (labeled 1 and 2).

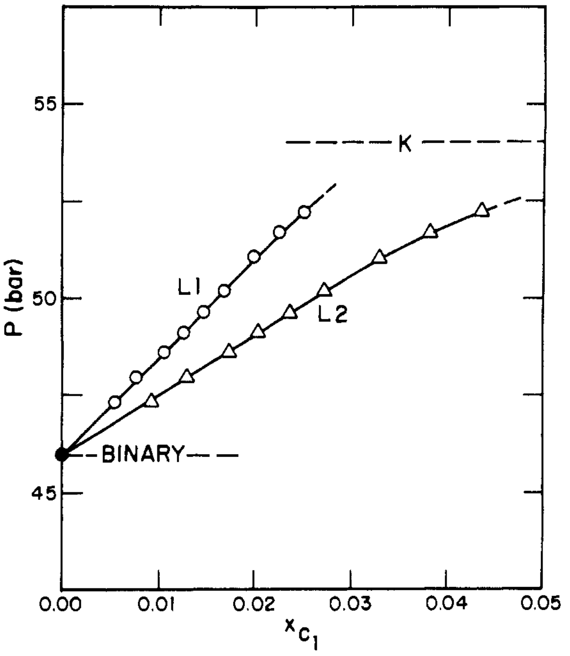

Figure 4. Methane mole fraction as a function of pressure for the L_1 and L_2 phases for the liquid–liquid–vapor region of methane + ethane + *n*-docosane at 30 °C.

balanced at their pressures, to be maintained throughout the run.

The liquid level is measured with the cathetometer, so that the volume of the vapor space can be known, since it initially contains the ethane at atmospheric pressure. In addition, the line from the regulating valves to the top of the visual cell also contains ethane at the same pressure as the visual cell. This line is carefully calibrated with respect to volume prior to the run and is kept at a constant known temperature.

An ethane addition is made slowly through valve RV1, with the pump RP1 being advanced at constant pressure to avoid adiabatic disturbances to the bomb MC1. The cell contents are stirred periodically during the course of the addition. The addition process proceeds until a trace amount of second liquid phase is observed. More ethane may be added to the cell to achieve the desired amount of each individual phase. The cell contents are then stirred for several minutes at a constant temperature, until the cell pressure stabilizes to ±0.1 psi. Valve V13 is then shut to separate the visual cell unit from the gas delivery system. The line from the regulating valves to valve

Table IV. Pressure, Phase Compositions, and Molar Volumes for the Liquid–Liquid–Vapor Region of Methane + Ethane + *n*-Tetradecylbenzene

press., bar	L_1 phase			L_2 phase			V phase	
	mole fracn		mol vol, mL/(g·mol)	mole fracn		mol vol, mL/(g·mol)	mole fracn	mol vol, mL/(g·mol)
	C_1	C_2		C_1	C_2		C_2	
Temperature = 5 °C (278.15 K)								
35.86[a]								
39.64	0.0650	0.8251	91.8	0.0918	0.8908	77.8	0.7598	343.2
41.37	0.0718	0.8080	93.9	0.1060	0.8799	78.0	0.7406	324.3
43.44	0.0791	0.7895	96.2	0.1232	0.8657	78.3	0.7195	303.8
45.51	0.0850	0.7731	98.6	0.1399	0.8512	78.9	0.6994	284.8
47.57	0.0918	0.7573	100.3	0.1563	0.8365	79.6	0.6803	267.8
49.64	0.0991	0.7415	102.1	0.1727	0.8213	80.3	0.6617	251.3
51.71	0.1056	0.7271	103.7	0.1899	0.8051	81.1	0.6486	235.6
53.78	0.1115	0.7145	105.2	0.2074	0.7882	82.6	0.6378	220.1
55.85	0.1177	0.7008	107.0	0.2241	0.7723	83.4	0.6272	206.4
57.92	0.1233	0.6881	108.6	0.2426	0.7544	85.3	0.6198	192.1
59.98	0.1290	0.6752	109.9	0.2655	0.7322	88.3	0.6151	176.9
62.05	0.1342	0.6637	111.0	0.2872	0.7110	92.0	0.6122	161.2
64.91[b]								
Temperature = 15 °C (288.15 K)								
36.48[a]								
39.71	0.0304	0.8669	93.6	0.0400	0.9419	80.2	0.8849	352.1
41.37	0.0370	0.8496	95.9	0.0519	0.9335	80.4	0.8617	331.6
43.44	0.0429	0.8322	98.6	0.0670	0.9212	81.0	0.8359	308.3
45.51	0.0505	0.8148	100.9	0.0823	0.9083	82.0	0.8147	285.3
47.57	0.0571	0.7985	102.8	0.0974	0.8950	83.1	0.7948	266.4
49.64	0.0632	0.7844	104.4	0.1144	0.8792	85.5	0.7826	237.2
52.40	0.0722	0.7651	106.8	0.1361	0.8590	87.5	0.7622	217.5
55.16	0.0828	0.7448	108.5	0.1571	0.8392	91.2	0.7475	196.0
57.92	0.0908	0.7277	110.7	0.1849	0.8122	95.0	0.7370	174.4
59.29	0.0945	0.7195	111.9	0.1990	0.7986	98.6	0.7344	161.7
61.29[b]								
Temperature = 25 °C (298.15 K)								
41.44[c]		0.8927	94.3		0.9867	85.0		
43.09	0.0052	0.8798	95.5	0.0093	0.9801	86.4	0.9827	274.2
44.13	0.0092	0.8711	96.4	0.0159	0.9745	87.1	0.9689	264.0
45.51	0.0144	0.8599	97.6	0.0251	0.9665	88.2	0.9519	251.5
46.88	0.0191	0.8493	98.8	0.0342	0.9585	89.2	0.9361	239.9
48.26	0.0240	0.8399	99.7	0.0432	0.9506	90.5	0.9217	228.6
48.95	0.0257	0.8354	100.3	0.0492	0.9451	91.5	0.9107	220.3
50.33	0.0303	0.8262	101.2	0.0596	0.9354	93.1	0.8982	209.0
57.71	0.0346	0.8170	102.3	0.0702	0.9256	95.1	0.8870	197.1
53.09	0.0387	0.8083	103.1	0.0813	0.9151	97.8	0.8779	184.9
54.47	0.0426	0.8005	103.9	0.0932	0.9040	101.3	0.8705	171.6
56.59[b]								

[a] LCEP point. [b] K point. [c] Interpolated binary data from Table V.

V13 is then flushed and evacuated by using the second gas, methane, and a vacuum pump. Methane from the bomb MC2 is gradually added into the line by simultaneously opening valve RV2 and advancing pump RP2. With a pressure of the methane-containing portion of the line slightly higher than that of the cell, valve V13 is slowly reopened to allow the addition of methane into the cell. The cell pressure can be increased by adding methane. At each cell pressure, the levels of the two liquid phases are measured.

Pressure, temperature, and volumetric data measured during the course of an experimental run allow one to calculate the overall composition inside the visual cell at a given state. By mass balances, the compositions and molar volumes of the three phases can be determined from "conjugate" measurements at a given temperature and pressure. For the ternary systems, conjugate measurements involve taking phase volume and overall composition raw data from three experimental runs in which each phase is in turn volumetrically dominant relative to the two other phases. The necessary conjugate experiments therefore are an L_1-dominant run, an L_2-dominant run, and a V-dominant run. Herein, the L_1 phase is that liquid phase richer in the heavy hydrocarbon and is denser than the L_2 phase. For a ternary three-phase system, an invariant point requires that both the temperature and the pressure be fixed. Along a given isotherm, raw data were taken at various pressures and then plotted. Smoothing these raw data allowed the selection of specific pressures at the given temperature for appropriate mass balance analysis of the conjugate experiments. These procedures were always repeated in order to provide a measure of the data reproducibility.

The computations required to obtain the compositions and molar volumes of the three phases are the same as those employed by Fall (*19*). Specifically, the three conjugate runs described above uniquely determine a set of three molar densities, one for each phase present, for any (and all) species at a given temperature and pressure. The entire set of these densities can be reexpressed as phase densities and mole fractions. An alternative data analysis approach is the least-squares procedure of Knobler and Scott (*20*); the results obtained by their method of analysis turned out to be quite similar to the results we report here (*21*).

The experimental procedure for the binary liquid–liquid–vapor system ethane + *n*-tetradecylbenzene is similar to that of the ternary system. For the binary system with three phases in equilibria at a specified temperature, the number of degrees of freedom is zero. The vapor phase in the binary experiments

Table V. Temperature, Pressure, Phase Composition, and Molar Volume Raw Data for the Liquid–Liquid–Vapor Locus of Ethane + *n*-Tetradecylbenzene

		L_1 phase		L_2 phase	
temp, K	press., bar	$[C_2]$, mole fracn	mol vol, mL/(g·mol)	$[C_2]$, mole fracn	mol vol, mL/(g·mol)
292.40	36.48[a]				
294.46	38.20	0.9137	89.6	0.9773	82.3
296.40	39.86	0.9017	92.3	0.9829	83.4
298.21	41.45	0.8930	94.4	0.9866	85.0
300.52	43.56	0.8831	96.6	0.9899	87.6
301.15	44.21	0.8798	97.7	0.9912	88.4
303.16	46.16	0.8722	99.5	0.9935	91.5
305.18	48.17	0.8648	101.5	0.9953	96.9
307.21	50.30	0.8599	101.5	0.9974	106.3
307.98	51.04[b]				

[a] LCEP point. [b] K point.

was assumed to be pure ethane, containing no *n*-tetradecylbenzene due to the low volatility of the hydrocarbon at the temperatures of interest. This assumption is discussed further in the Remarks. Thus, conjugate measurements were made using only L_1-dominant and L_2-dominant experimental runs to obtain the properties of the L_1 and L_2 phases. The boundaries of the LLV region for the ternary systems and the end points of the LLV locus for the binary system were determined by straightforward visual observation.

Temperature was measured with Pt-resistant thermometer to an estimated accuracy of ±0.02 K. Pressure was measured to ±0.07 bar with pressure transducers which were frequently calibrated with a dead-weight gauge. Phase volumes in the calibrated visual cell were determined by a cathetometer to an accuracy of ±0.005 mL.

Materials

n-Docosane and *n*-tetradecylbenzene were purchased from Alfa Products with stated purities of 99 and 97%, respectively. The air-saturated melting point of *n*-docosane was determined to be 43.59 ± 0.05 °C. This value compares favorably with the value of 43.70 °C reported by Estrera and Luks (*10*). The melting point of *n*-tetradecylbenzene was determined to be 9.68 ± 0.05 °C.

The ethane was obtained from the Matheson Co. as a research purity grade gas with a minimum purity rating of 99.93 mol %. The difference between the bubble point and dew point at 25 °C was less than 0.07 bar, and the vapor pressure at 50% liquid phase by volume was within ±0.07 bar of the literature value (*22*). The critical point of ethane was determined to be 48.81 bar and 32.18 °C, comparing favorably with that reported in the literature (*23*). The ethane was first liquefied in an evacuated storage bomb cooled down to approximately 0 °C. In this two-phase condition, the vapor phase was vented and discarded to remove any light impurities.

The methane was obtained from Union Carbide Corp., Linde Division, as ultrahigh purity with a minimum rating of 99.97%. No further purification of *n*-docosane, *n*-tetradecylbenzene, and methane was performed.

Results

Tables I and II present pressure and temperature data for the LCEP (L=L–V), Q(SLLV)-point, and K(L–L=V)-point loci which bound the three-phase LLV regions of the mixture methane + ethane + *n*-docosane and the mixture methane + ethane + *n*-tetradecylbenzene, respectively. Figure 3 shows these data in *P–T* space, along with the constituent binary LLV loci, superimposed on the pure gas solvent component vapor pressures (*22*, *24*) and the critical locus for the mixture methane + ethane (*25*). These LCEP, Q-point and K-point data should be good to ±0.06 K and ±0.07 bar. The intersections of the three-phase boundary loci in Figure 3 are not directly measured and should be considered as estimates.

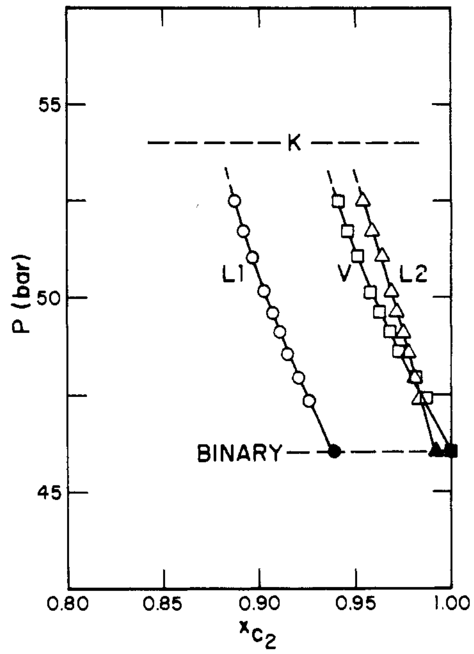

Figure 5. Ethane mole fraction as a function of pressure for all the phases of the liquid–liquid–vapor region of methane + ethane + *n*-docosane at 30 °C.

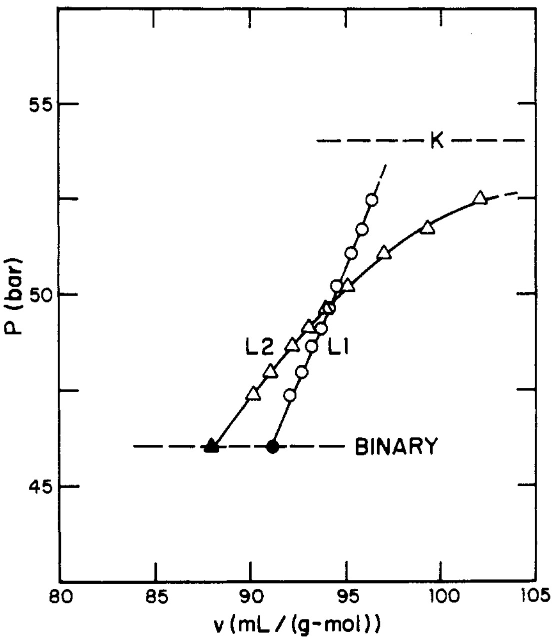

Figure 6. Molar volumes as a function of pressure for the L_1 and L_2 phases for the liquid–liquid–vapor region of methane + ethane + *n*-docosane at 30 °C.

The LLV data for the methane + ethane + *n*-docosane system for isotherms at 25 and 30 °C are presented in Table III. The molar compositions are estimated to be good to ±0.003 and the liquid-phase molar volumes good to ±1.5 mL/(g·mol) at 25 °C. For the 30 °C isotherm, the molar compositions should be good to ±0.002 and the liquid-phase molar volumes good to ±0.5 mL/(g·mol). Vapor-phase molar volumes for both isotherms should be reliable to ±1.0% of the reported

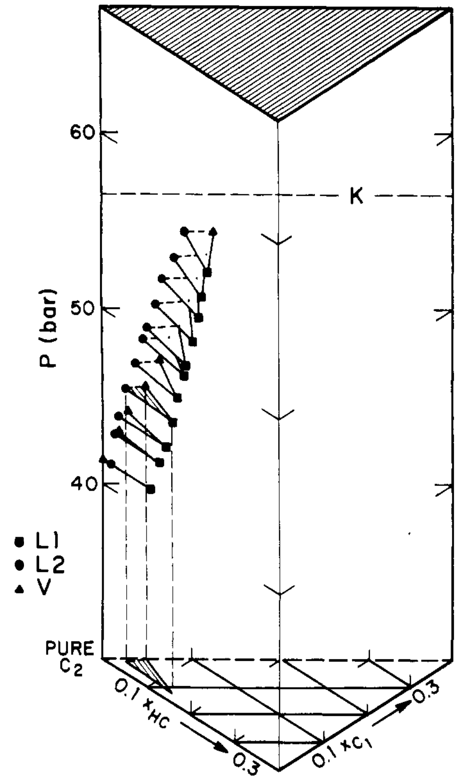

Figure 7. Compositional ternary diagram for the liquid-liquid-vapor region of methane + ethane + *n*-tetradecylbenzene at 25 °C.

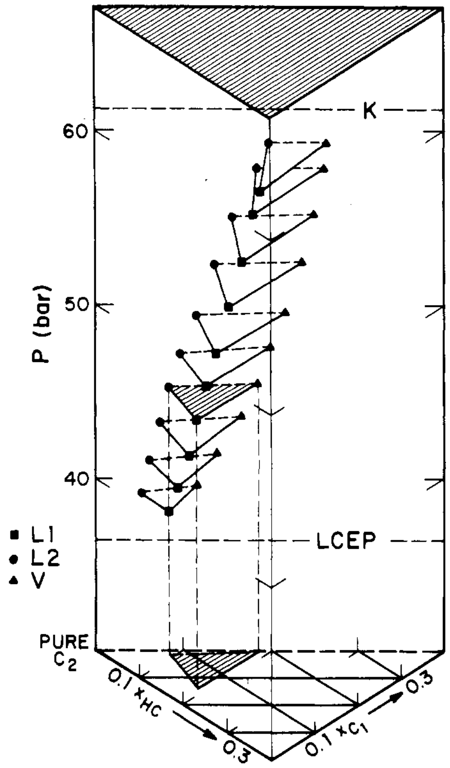

Figure 8. Compositional ternary diagram for the liquid-liquid-vapor region of methane + ethane + *n*-tetradecylbenzene at 15 °C.

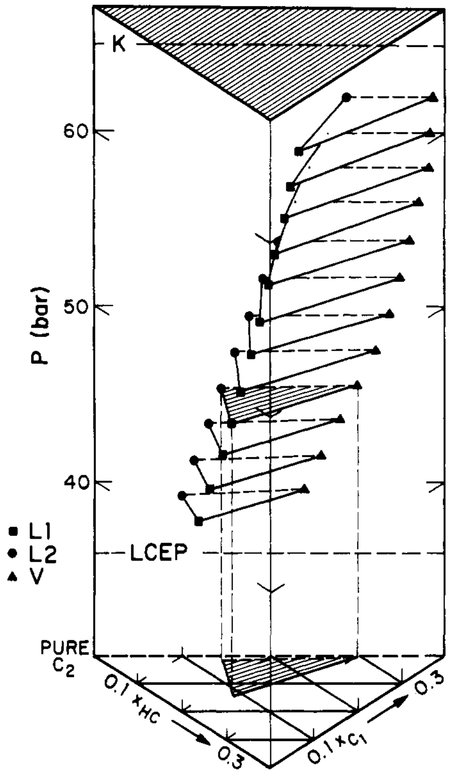

Figure 9. Compositional ternary diagram for the liquid-liquid-vapor region of methane + ethane + *n*-tetradecylbenzene at 5 °C.

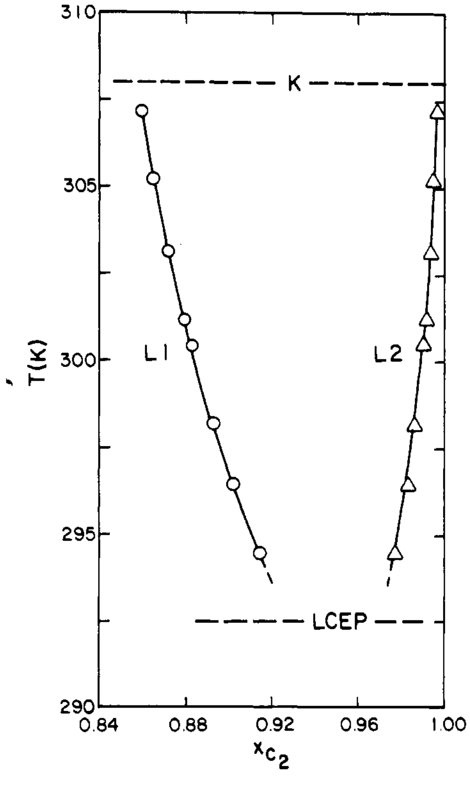

Figure 10. Composition as a function of temperature for the L_1 and L_2 phases for the liquid-liquid-vapor locus of ethane + *n*-tetradecylbenzene.

values at all pressures. The improvement in the results with increasing temperature may be due to the reduced chance of solid *n*-docosane deposits forming in certain parts of the cell such as the capillary neck portion, even though such deposits were not visually observed by the investigators. A similar phenomenon was suggested to explain for uneven data reproducibility in the ethane + propane + *n*-dotriacontane ternary mixture study of Estrera and Luks (*26*).

Table IV presents the LLV data for the methane + ethane + *n*-tetradecylbenzene system for isotherms at 5, 15, and 25 °C. The molar compositions should be good to ±0.002 and the

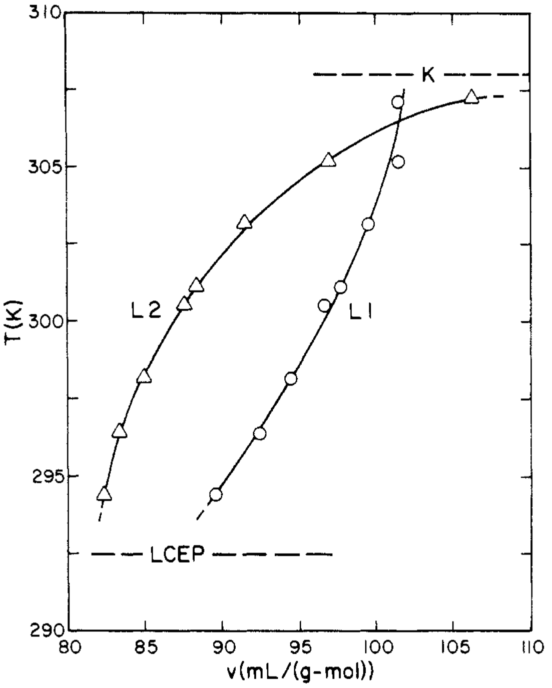

Figure 11. Molar volume as a function of temperature for the L_1 and L_2 phases for the liquid–liquid–vapor locus of ethane + *n*-tetradecylbenzene.

liquid-phase molar volumes good to ±0.6 mL/(g·mol) at all temperatures. Vapor-phase molar volumes should be within ±1.2% of the reported values at all pressures.

Table V presents raw data for the LLV locus of the binary mixture ethane + *n*-tetradecylbenzene, including composition and molar volume for each of the liquid phases present. The compositions of the liquid phases for this system should be good to ±0.001 and the liquid-phase molar volumes good to ±0.4 mL/(g·mol). All the estimates for the ternary and binary systems are based on average absolute deviations (AAD) of the raw LLV data, of several experimental runs, from smoothed curves of the data; we consider these estimates to be conservative.

Plots of LLV behavior of the methane + ethane + *n*-docosane system at 30 °C are presented in Figures 4–6. Figures 4 and 5 present liquid- and vapor-phase compositions as functions of pressure, while Figure 6 presents the liquid-phase molar volumes versus pressure. Figures 7–9 show the LLV compositional ternary diagrams as functions of pressure along the isotherms at 25, 15, and 5 °C of the system methane + ethane + *n*-tetradecylbenzene. Figures 10 and 11 show the L_1 and L_2 compositions and molar volumes plotted against temperature for the ethane + *n*-tetradecylbenzene binary system.

Remarks

The LLV immiscibility behavior seen in the two ternary systems was qualitatively as anticipated. The addition of methane to the constituent immiscible binary mixtures (ethane + *n*-docosane and ethane + *n*-tetradecylbenzene, respectively) resulted in a three-phase region expanding in the direction of the vapor pressure curve of methane from the binary LLV locus (boundary). These two ternary systems are topographically similar sharing the same type of LLV region boundaries (K-point, Q-point, LCEP, and binary LLV loci). The K-point boundaries of the two LLV regions are located close to the critical point locus (L=V) of the binary mixture methane + ethane, since the L_2 and V phases of the ternary systems are compositionally similar to the binary LV system of methane + ethane at corresponding temperatures and pressures. The solubility of the heavy hydrocarbons in the L_2 phase is typically on the order of 1 mol %.

The immiscibility region of the methane + ethane + *n*-tetradecylbenzene system is much wider than that of the methane + ethane + *n*-docosane system. This larger LLV region can be accounted for by the fact that the melting point of *n*-tetradecylbenzene is significantly lower than that of *n*-docosane, therefore causing the LLV region of the methane + ethane + *n*-tetradecylbenzene system to extend to lower temperatures than the system methane + ethane + *n*-docosane before the solid-phase formation of solute (heavy hydrocarbon) as a four-phase SLLV locus occurs.

In these two ternary mixtures, methane resides predominantly in the vapor phase, especially at lower temperatures. This can be observed from the ternary diagrams shown in Figures 7–9. Methane and ethane are also found to be less soluble in the L_1 phase for the system methane + ethane + *n*-tetradecylbenzene than for the system methane + ethane + *n*-docosane at the same temperature and pressure, as would be expected for an aromatic hydrocarbon versus a paraffinic hydrocarbon.

One comment should be made about the amount of the solutes (*n*-docosane and *n*-tetradecylbenzene) in the vapor phase for these two ternary systems. The mass-balance calculations for the ternary three-phase systems were based on the assumption that there was not any solute component present in the vapor phase. Hence, only the amount of the two solvent gases in the vapor phase were calculated. This assumption was made due to the relatively low vapor pressure of the solutes in question at the temperatures of interest. However, if the mass-balance calculations are performed without such an assumption, the mole fraction of solutes in the vapor phase for the two ternary systems in this study are found to be in the range of 0.0002–0.0009, ±50%, and do not significantly affect the numerical values of the properties presented in this paper (*21*).

Glossary

AAD	average absolute deviation
C_1	methane
C_2	ethane
K	a K point, a critical end point where L–L=V
L, L_1, L_2	liquid phases
LCEP	a lower critical end point where L=L–V
Q	a Q point, or quadruple point, which has four phases in equilibria; herein, the four phases are SLLV
S	solid phase
V	vapor phase

Registry No. C_1, 74-82-8; C_2, 74-84-0; *n*-docosane, 629-97-0; *n*-tetradecylbenzene, 1459-10-5.

Literature Cited

(1) Lin, Y. N.; Chen, R. J. J.; Chappelear, P. S.; Kobayashi, R. *J. Chem. Eng. Data* **1977**, *22*, 402–408.
(2) Kohn, J. P. *AIChE J.* **1961**, *7*, 514–518.
(3) Chang, H. L.; Hurt, L. J.; Kobayashi, R. *AIChE J.* **1966**, *12*, 1212–1216.
(4) Luks, K. D.; Kohn, J. P. *Proceedings of the 63rd Annual Convention Gas Processors Association, New Orleans, LA, March 21, 1984*; Gas Processors Association: Tulsa, OK, 1984; pp 181–186.
(5) Kohn, J. P.; Kim, Y. J.; Pan, Y. C. *J. Chem. Eng. Data* **1966**, *11*, 333–335.
(6) Specovius, J.; Leiva, M. A.; Scott, R. D.; Knobler, C. M. *J. Phys. Chem.* **1981**, *85*, 2313–2316.
(7) Rodrigues, A. B.; Kohn, J. P. *J. Chem. Eng. Data* **1967**, *12*, 191–193.
(8) Patel, A. D. M.S. Thesis, University of Notre Dame, Notre Dame, IN, August 1966.
(9) Peters, C. J.; Lichtenthaler, R. N.; de Swaan Arons, J. *Fluid Phase Equilib.* **1986**, *29*, 495–504.
(10) Estrera, S. S.; Luks, K. D. *J. Chem. Eng. Data* **1987**, *32*, 201–204.

(11) Peters, C. J.; de Roo, J. L.; de Swaan Arons, J. *J. Chem. Thermodyn.* **1987**, *19*, 265–272.
(12) Peters, C. J.; Van Der Kooi, H. J.; de Swaan Arons, J. *J. Chem. Thermodyn.* **1987**, *19*, 395–405.
(13) Jangkamolkulchai, A.; Arbuckle, M. M.; Luks, K. D. *Fluid Phase Equilib.* **1988**, *40*, 235–245.
(14) Miller, M. M.; Luks, K. D. *Fluid Phase Equilib.*, in press.
(15) Luks, K. D. *Fluid Phase Equilib.* **1986**, *29*, 209–224.
(16) Fall, D. J.; Luks, K. D. *J. Chem. Eng. Data* **1984**, *29*, 413–417.
(17) Fall, D. J.; Fall, J. L.; Luks, K. D. *J. Chem. Eng. Data* **1985**, *30*, 82–88.
(18) Fall, J. L.; Luks, K. D. *J. Chem. Eng. Data* **1986**, *31*, 332–336.
(19) Fall, J. L. Ph.D. Dissertation, University of Tulsa, Tulsa, OK, 1985.
(20) Knobler, C. M.; Scott, R. L. *J. Chem. Phys.* **1980**, *73*, 5390–5391.
(21) Jangkamolkulchai, A. Ph.D. Dissertation, University of Tulsa, Tulsa, OK, 1988.
(22) Goodwin, R. D.; Roder, H. M.; Straty, G. C. *NBS* **1976**, *Note No. 684*, 58–61.
(23) Weast, R. C. *Handbook of Chemistry and Physics*, 51st ed.; The Chemical Rubber Co.: Boca Raton, FL, 1970; p D-148.
(24) Angus, S.; Armstrong, B.; de Reuck, K. M. *International Thermodynamic Tables of the Fluid State-5 Methane*; Pergamon: 1976; pp 240–241.
(25) Price, A. R.; Kobayashi, R. *J. Chem. Eng. Data* **1959**, *4*, 40–52.
(26) Estrera, S. S.; Luks, K. D. *J. Chem. Eng. Data* **1988**, *33*, 350–354.

Received for review April 1, 1988. Accepted July 26, 1988. Support of this research was provided by the National Science Foundation (Grant CBT-8715965). The apparatus used is part of the PVTx Laboratory at The University of Tulsa and was purchased with funds provided by several industries, The University of Tulsa, and a National Science Foundation specialized equipment grant (CPE-8104650).

Thermodynamic Functions and Vapor Pressures of Triphenylphosphine Oxide and 1,4-Bis(diphenylphosphino)butane Near the Melting Point

Jan Huinink,* Kees van Miltenburg, Harry A. J. Oonk, and Abraham Schuijff

Chemical Thermodynamics Group, University of Utrecht, Transitorium III, Padualaan 8, De Uithof, 3584 CH Utrecht, The Netherlands

Paul Groen

Department of Chemical Technology, Delft University of Technology, Julianalaan 136, 2628 BL Delft, The Netherlands

The enthalpies of vaporization/sublimation were derived from the temperature dependence of vapor pressures measured by the technique of simultaneous torsion and mass loss effusion in the pressure region of 0.1–1 Pa. In addition, specific heats and heats of fusion were determined by DTA. The results for triphenylphosphine oxide (solid) are $\Delta H^\circ_v(398.86\ \mathrm{K}) = 131.0 \pm 2\ \mathrm{kJ\ mol^{-1}}$, $\Delta G^\circ_v(398.86\ \mathrm{K}) = 3039 \pm 100\ \mathrm{J\ mol^{-1}}$, $p(398.86\ \mathrm{K}) = 0.4 \pm 0.01\ \mathrm{Pa}$, $\Delta H^\circ_f(429.6\ \mathrm{K}) = 23.4 \pm 0.25\ \mathrm{J\ mol^{-1}}$, $C_p^\circ(404.0\ \mathrm{K}) = 431 \pm 3\ \mathrm{J\ mol^{-1}\ K^{-1}}$, and $C_p^\circ(444.0\ \mathrm{K}) = 527 \pm 5\ \mathrm{J\ mol^{-1}\ K^{-1}}$. The results for 1,4-bis(diphenylphosphino)butane (liquid) are $\Delta H^\circ_v(443.22\ \mathrm{K}) = 126.3 \pm 2\ \mathrm{kJ\ mol^{-1}}$, $\Delta G^\circ_v(443.22\ \mathrm{K}) = 3377 \pm 100\ \mathrm{J\ mol^{-1}}$, $p(443.22\ \mathrm{K}) = 0.4 \pm 0.01\ \mathrm{Pa}$, $\Delta H^\circ_f(405.9\ \mathrm{K}) = 45.3 \pm 0.5\ \mathrm{KJ\ mol^{-1}}$, $C_p^\circ(384.0\ \mathrm{K}) = 384 \pm 4\ \mathrm{J\ mol^{-1}\ K^{-1}}$, and $C_p^\circ(429.0\ \mathrm{K}) = 520 \pm 5\ \mathrm{J\ mol^{-1}\ K^{-1}}$.

Introduction

Hydridocarbonyltris(triphenylphosphine)rhodium (I) dissolved in suitable solvents is being used as a heterogeneous catalyst in the hydroformylation of propylene. Because the catalyst is applied in large-scale chemical reactors and decomposes when the solvent has evaporated, it is necessary to use solvents having low vapor pressures under reaction conditions.

Knowledge of the vapor pressures of the pure substances as a function of the temperature is required to calculate the vaporization losses of the solvents in the reaction mixture in the reactor. Three suitable solvents, triphenyl-, tri-*p*-tolyl-, and tris(2-cyanoethyl)phosphine have been studied by de Kruif, Herman, and van den Berg (*1*).

The vapor pressures of two further solvents are presented in this paper. For the purpose of extrapolation of the vapor pressures of triphenylphosphine oxide to the temperature region of the supercooled liquid, needed for the calculation of losses in the reactor, the melting heat and specific heats of this compound are also measured; for completeness the values for the butane compound are also given.

Experimental Section

Samples. Triphenylphosphine oxide (TPPO), obtained from Merck (West Germany), purity >98%, and 1,4-bis(diphenylphosphino)butane (BDPPB), obtained from Ventron (West Germany), purity >98%, were used without further purification because the measured vapor pressure of the compounds did not change significantly with loss of mass during the measurements.

The vapor pressure measurements were carried out with a simultaneous torsion and mass loss effusion apparatus as described in an earlier paper (de Kruif et al. (*2*)). The effusion cell is provided with two orifices 1 mm in diameter made in 6-μm platinum foil and are positioned 20 mm apart on opposite sides of the cell. The torsion effusion method measures the pressure as a recoil force (the rate of loss of momentum from the holes) and does not depend on the mass of the effusing molecules. In the mass loss effusion method the pressure is calculated from the rate of mass loss and depends on the mass of the effusing molecules by a factor $m^{-1/2}$. Decomposition of the sample or dimerization in the gas phase is easily recognized by comparison of the pressures measured by both methods. The calibration was done with naphthalene (Ambrose et al. (*3*)). The measuring procedure was started at a temperature corresponding with a vapor pressure of about 0.15 Pa. Five measurements at 30-s intervals were made followed by an increase of the oven temperature of about 0.9 K. The temperature of the sample was measured with a thermistor, calibrated on IPTS-68, positioned in the middle of the effusion cell. In order to allow the cell to come into temperature equilibrium with the surrounding oven, a period of 20 min was observed between the successive series of measurements. The procedure was continued until the pressure was about 1 Pa, giving a set of

0021-9568/89/1734-0099$01.50/0 © 1989 American Chemical Society